

**Energy storage performance in NaNbO_3 lead-free dielectric
ceramics by doping $\text{Sr}(\text{Mg}_{1/3}\text{Sb}_{2/3})\text{O}_3$**

Qinpeng Dong, Peng Nong, Yue Pan , Dafu Zeng, Mingzhao Xu, Huanfu Zhou, Xu Li¹,

Xiuli Chen²

Key Laboratory of Nonferrous Materials and New Processing Technology,

Ministry of Education, School of Materials Science and Engineering, Guilin

University of Technology, Guilin 541004, China.

¹ Corresponding author. E-mail address: lx100527@163.com

² Corresponding author. E-mail address: cxlnwpu@163.com

1. Experimental

$(1-x)\text{NaNbO}_3-x\text{Sr}(\text{Mg}_{1/3}\text{Sb}_{2/3})\text{O}_3$ ($x = 0.07, 0.10, 0.13, 0.16$) was prepared by a conventional solid-state reaction. Na_2CO_3 (99.8%), Sr_2CO_3 (99%), Nb_2O_5 (99%) and MgO (98.5%), Sb_2O_3 (99%) were stoichiometrically weighed and ball-milled with zirconium balls in ethanol for 5 hours. After drying, the mixed powders are calcined at 950°C for 5 hours and ball milled again for 5 hours. Polyvinyl alcohol was added as a binder to press the dried powder into a disc with a diameter of 8 mm and a thickness of 2 mm. Finally, the precursor powder of the same composition was embedded in the sample and sintered at 1365°C for 3 hours.

2. Characterization

Sample characterization: X-ray powder diffraction (XRD, model X'Pert PRO; PANalytical, Almelo, The Netherlands) using $\text{Cu K}\alpha$ radiation ($\lambda = 0.15406$ nm) was used to analyse the phase structure of the samples. A scanning electron microscope (model GeminiSEM 300, OXIG, Oxfordshire, UK) was used to observe the microstructure of the samples. The selected area electron diffraction (SAED) and TEM morphology were acquired by JEM-2100F. Raman shifts were measured at room temperature with a Raman tester (XDR), (XDR, Thermo Fisher Scientific, USA) was used. Using X-ray photoelectron spectroscopy (XPS) for qualitative analysis and quantitative analysis, (ESCALAB250 Xi, TMO, USA). The relative permittivity and loss tangent of the ceramics were measured using a precision impedance analyser (Model 4294A, Hewlett-Packard Co, Palo Alto, CA) in the temperature range of -196°C to 300°C and 400°C to 600°C with the heating rate of $2^\circ\text{C}/\text{min}$. To further investigate the energy

storage properties, the sintered samples were polished to a thickness of 0.1 ± 0.01 mm and coated with a 2 mm diameter ceramic. and coated with a silver paste of 2 mm in diameter (area of 3.14 mm^2). The temperature was increased to 700°C and then held for 30 minutes at a heating rate of 3°C . Oven and then held at a heating rate of 3°C per minute for 30 minutes to make a simple parallel plate capacitor for P - E loop testing. A simple parallel plate capacitor was fabricated for P - E loop testing (Ferroelectric Material Parameter Tester (RT66, Radiant Technologies, NM, USA)). Dielectric breakdown strength (E_b) was tested at room temperature using a voltage-endurance test set. (Dielectric Charge Test System (CFD-003, TG Technologies, Shanghai, China)) was used to measure the charging/discharging properties.

3. Results and discussion

In order to further study the dielectric properties of NN-SMSb ceramics, the dielectric constant of ceramics was tested at different temperatures and frequencies. The results are shown in Fig. S 2 (a)-(d). There are two peaks in 0.07NN-SMSb ceramic at -100°C and 200°C , corresponding to the ferroelectric-paraelectric phase transition point (T_a) and the ferroelectric-ferroelectric phase transition point (T_m), respectively [1-4]. The double peaks may be caused by the phase transition from paraelectric phase to monoclinic phase. A similar phenomenon was found in 0.9NaNbO_3 - $0.1\text{Bi}(\text{Mg}_{2/3}\text{Sb}_{1/3})\text{O}_3$ ceramic prepared by chen et al [5, 6]. When $x \leq 0.10$, the T_m peak of the ceramics gradually moves to the high temperature direction with the increase of frequency, showing a typical medium diffusion behavior [4, 7, 8]. However, due to the limitation of instrument temperature, NN-SMSb ceramics did not show T_m peak at -160

°C to 250 °C when $x \geq 0.13$, The existing data are processed by the formula [9]:

$$\frac{1}{\varepsilon_r} - \frac{1}{\varepsilon_m} = \frac{(T - T_m)\gamma}{C}$$

(C , T_m , γ , which represent Curie constant, temperature and dispersion coefficient corresponding to ε_m , respectively), and the calculation results are

shown in **Fig. S 2 (e)**. **Fig. S 2 (f)** shows the frequency spectrum of NN–SMSb ceramics.

The results show that the dielectric constant and loss of ceramics do not change significantly with the increase of frequency, indicating that NN–SMSb ceramics are less sensitive to frequency changes and have good frequency stability.

The charge/discharge test results of 0.13NN–SMSb ceramic are shown in **Fig. S 3** is the overdamped charge/discharge curve of the ceramic at room temperature. The results show that the discharge current gradually increases from 1.14 A to 10.35 A. In order to characterize the discharge capacity of the ceramic in practical applications, the discharge rate of the ceramic was evaluated by $t_{0.9}$, that is, the time required for ceramic to release 90 % energy, as shown in **Fig. S 3 (b)**. The $t_{0.9}$ of the ceramic is about 105.5 ns, which has a high discharge rate. This can be attributed to the rapid response of the polar–nano regions (PNRs) formed by the substitution of ions in the ceramic to the electric field. The underdamped charge/discharge test curve of the ceramic is shown in **Fig. S 4**. With the increase of E , the discharge current of the ceramic increased from 11.4 A to 71.5 A, and the power density P_D and current density C_D increased from 1.61 MW/cm³ and 161.36 A/cm³ to 101.16 MW/cm³ and 1011.56 A/cm³, respectively. The results shows that 0.13NN–SMSb ceramic have a fast discharge rate, and have broad application prospects in pulse power systems.

Fig. S 5 shows the P – E loop of 0.13NN–SMSb ceramic at different temperatures

and frequencies. With the increase of temperature, the P_{\max} and P_r of ceramic gradually increase. The increase of P_{\max} may be due to the decrease of the reversal electric field of some PNRs at high temperature. The increase of P_r can be attributed to the increase of oxygen vacancy concentration and conductivity at high temperature [10, 11]. At 40 – 140 °C, the ΔP of the ceramic decreased from 17.80 $\mu\text{C}/\text{cm}^2$ to 16.33 $\mu\text{C}/\text{cm}^2$ with a change rate of less than 8.3 %. At 10–120 Hz, the P_{\max} of the ceramic decreases from 19.32 $\mu\text{C}/\text{cm}^2$ to 18.32 $\mu\text{C}/\text{cm}^2$, and the change rate is less than 5.2 %. The results shows that the 0.13NN–SMSb ceramic have good frequency stability and temperature stability.

References

- [1] X. Wang, H. Chen, Y. Pan, Q. Dong, J. Wang, X. Chen, H. Zhou, Dielectric ceramics with excellent energy storage properties were obtained by doping 0.92NaNbO₃-0.08Bi(Ni_{0.5}Zr_{0.5})O₃ ceramics, *J. Power Sources* 566 (2023).
- [2] H. Chen, X. Chen, J. Shi, C. Sun, X. Dong, F. Pang, H. Zhou, Achieving ultrahigh energy storage density in NaNbO₃-Bi(Ni_{0.5}Zr_{0.5})O₃ solid solution by enhancing the breakdown electric field, *Ceram. Int.* 46(18) (2020) 28407-28413.
- [3] A. Xie, J. Fu, R. Zuo, C. Zhou, Z. Qiao, T. Li, S. Zhang, NaNbO₃-CaTiO₃ lead-free relaxor antiferroelectric ceramics featuring giant energy density, high energy efficiency and power density, *Chem. Eng. J.* 429 (2022).
- [4] X. Li, X. Dong, F. Wang, Z. Tan, Q. Zhang, H. Chen, J. Xi, J. Xing, H. Zhou, J. Zhu, Realizing excellent energy storage properties in Na_{0.5}Bi_{0.5}TiO₃-based lead-free relaxor ferroelectrics, *J. Eur. Ceram. Soc.* 42(5) (2022) 2221-2229.
- [5] H. Chen, X. Dong, X. Wang, Y. Pan, J. Wang, L. Deng, X. Chen, Q. Dong, H. Zhang, H. Zhou, Energy storage properties in Bi(Mg_{1/2}Sb_{2/3})O₃-doped NaNbO₃ lead-free ceramics, *Ceram. Int.* 48(6) (2022) 7723-7729.
- [6] N. Qu, H. Du, X. Hao, A new strategy to realize high comprehensive energy storage properties in lead-free bulk ceramics, *J. Mater. Chem. C* 7(26) (2019) 7993-8002.
- [7] X. Dong, X. Li, X. Chen, Z. Tan, J. Wu, J. Zhu, H. Zhou, (1-x)[0.90NN-0.10Bi(Mg_{2/3}Nb_{1/3})O₃]-x(Bi_{0.5}Na_{0.5})_{0.7}Sr_{0.3}TiO₃ ceramics with core-shell structures: A pathway for simultaneously achieving high polarization and breakdown strength, *Nano Energy* 101 (2022).
- [8] L. Zhang, Z. Yan, T. Chen, H. Luo, H. Zhang, T. Khanom, D. Zhang, I. Abrahams, H. Yan, Tunable phase transitions in NaNbO₃ ceramics through bismuth/vacancy modification, *J. Mater. Chem. C* 9(12) (2021) 4289-4299.
- [9] H. Chen, J. Shi, X. Chen, C. Sun, F. Pang, X. Dong, H. Zhang, H. Zhou, Excellent energy storage properties and stability of NaNbO₃-Bi(Mg_{0.5}Ta_{0.5})O₃ ceramics by introducing (Bi_{0.5}Na_{0.5})_{0.7}Sr_{0.3}TiO₃, *J. Mater. Chem. A* 9(8) (2021) 4789-4799.
- [10] X. Gan, H. Yang, Y. Lin, J. Li, Improving the energy storage performances of Bi(Ni_{0.5}Ti_{0.5})O₃-added K_{0.5}Na_{0.5}NbO₃-based ceramics, *Ceram. Int.* (2022).
- [11] F. Pang, X. Chen, C. Sun, J. Shi, X. Li, H. Chen, X. Dong, H. Zhou, Ultrahigh Energy Storage Characteristics of Sodium Niobate-Based Ceramics by Introducing a Local Random Field, *ACS Sustain. Chem. Eng.* 8(39) (2020) 14985-14995.

Figure captions

Fig. S 1 : (a)–(d) is SEM image of NN–SMSb ceramics, (e) is elemental spectra of 0.13NN–SMSb ceramic.

Fig. S 2 : (a)–(d) are the thermogram of $x = 0.07, 0.10, 0.13, 0.16$ NN–SMSb ceramics, respectively, (e) γ values of the NN–SMSb ceramics, (f) spectrum of NN–SMSb ceramics.

Fig. S 3 : Overdamped charge/discharge waveforms of 0.13NN–SMSb ceramic at room temperature, (b) W_{dis} versus time at different E , (c) discharge current, W_{dis} and $t_{0.9}$ versus E .

Fig. S 4 : (a) Underdamped charge/discharge waveforms of 0.13NN–SMSb ceramic at room temperature, (b) P_D , C_D , and discharge current versus the E .

Fig. S 5 : (a) P – E loops at 40–140°C, (b) variation of P_{max} , P_r and ΔP with temperature at 40–140°C, (c) P – E loops at 10–120 Hz, (d) variation of P_{max} , P_r and ΔP with frequency at 10–120 Hz.

Fig. S 6 : (a) XRD Rietveld refinement results of 0.07NN–SMSb and 0.10NN–SMSb ceramic at 36–41°, (b) XRD Rietveld refinement results of 0.13NN–SMSb and 0.16NN–SMSb ceramic at 35.8–40.5°.

Figure

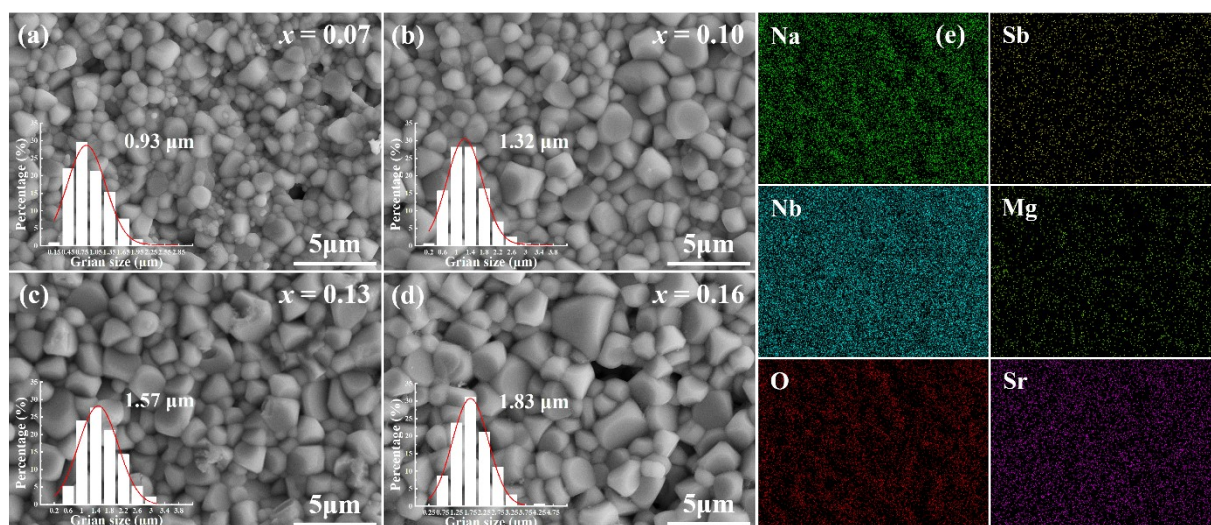


Fig. S 1

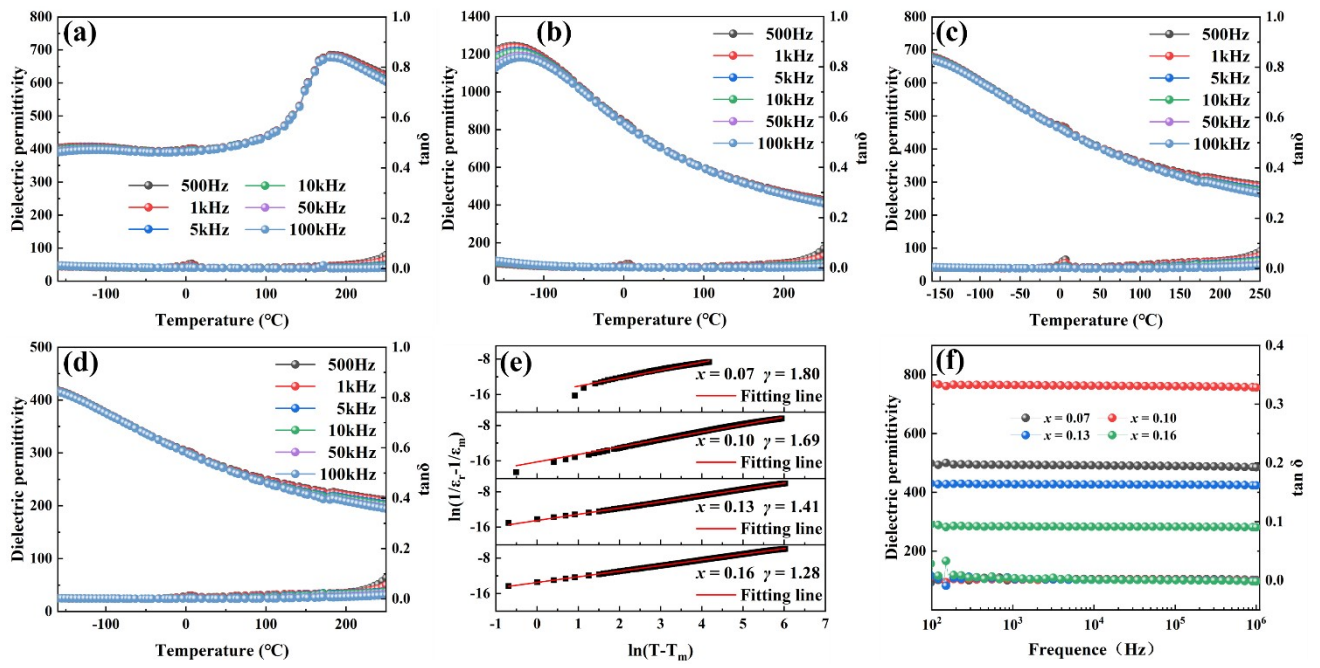


Fig. S 2

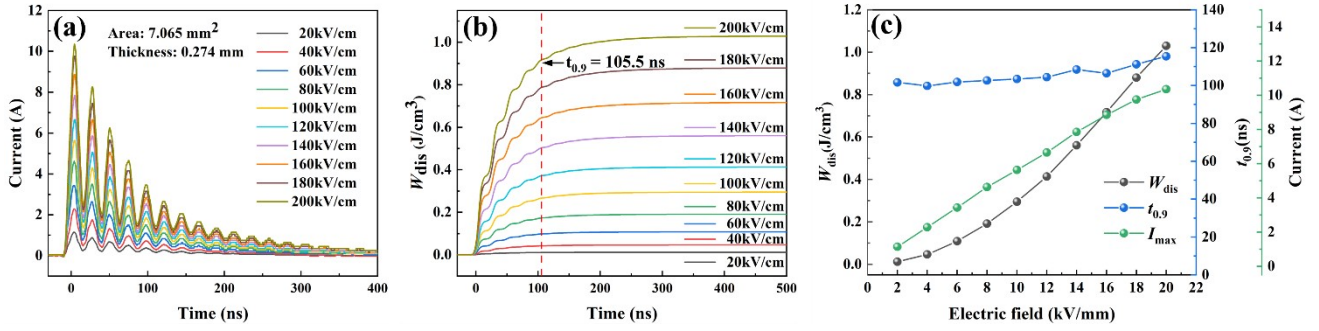


Fig. S 3

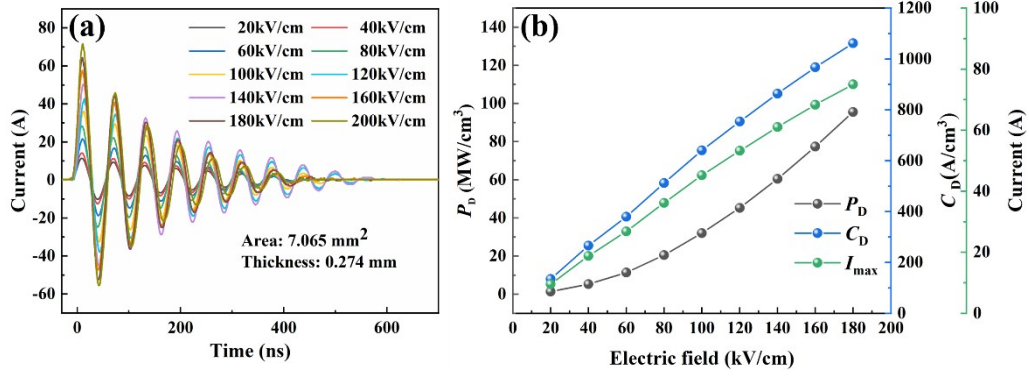


Fig. S 4

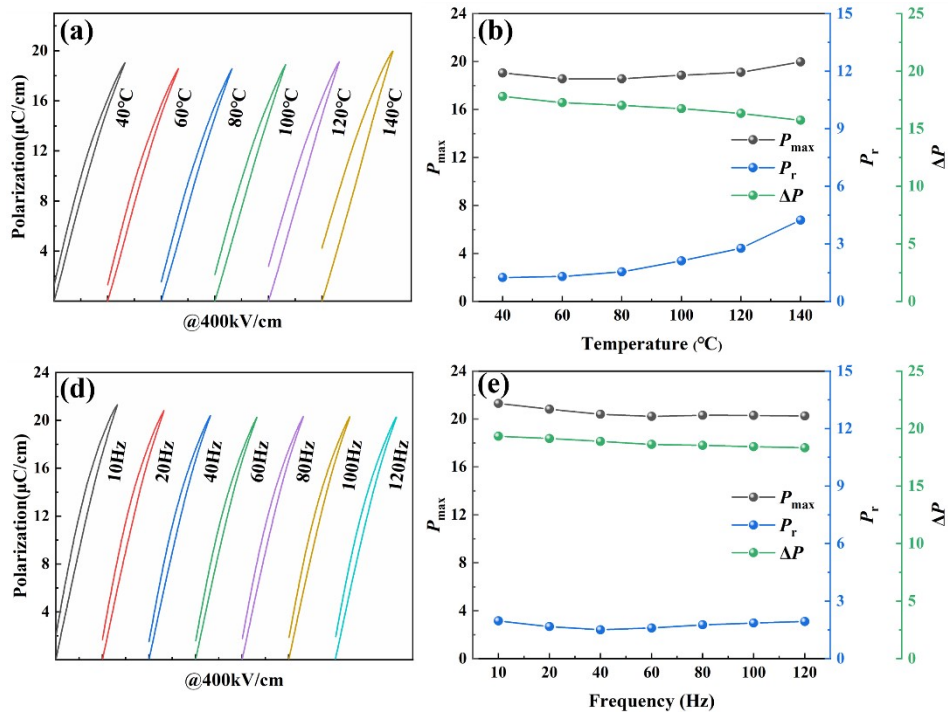


Fig. S 5

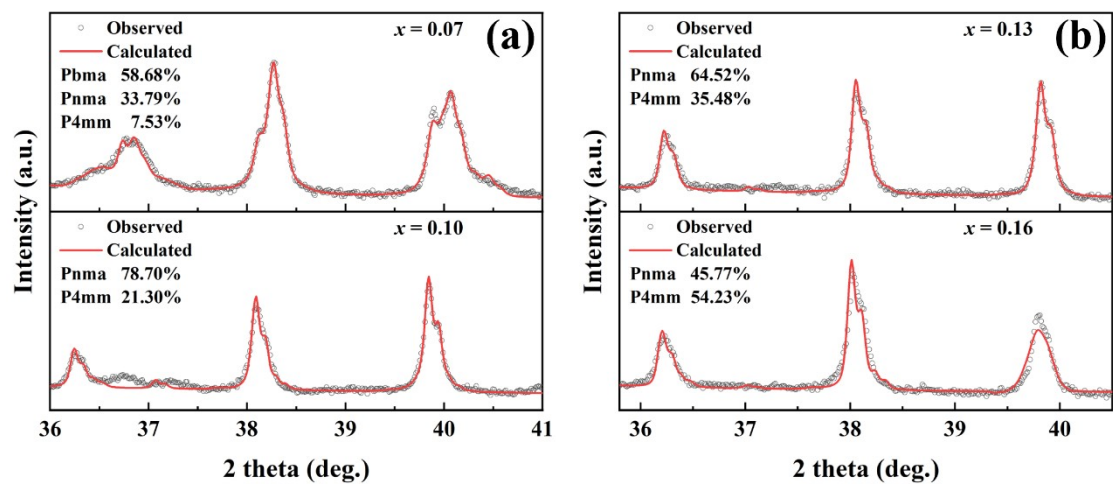


Fig. S 6